Serum Amyloid A Directly Accelerates the Progression of Atherosclerosis in Apolipoprotein E–Deficient Mice

Zhe Dong,[1] Tingting Wu,[1*] Weidong Qin,[1] Chuankai An,[2] Zhihao Wang, Mingxiang Zhang,[1] Yun Zhang,[1] Cheng Zhang,[1] and Fengshuang An[1]*

[1]Key Laboratory of Cardiovascular Remodeling and Function Research, Chinese Ministry of Education and Chinese Ministry of Health, Shandong University Qilu Hospital, Jinan, Shandong, China; [2]School of Electronics Engineering and Computer Science, Peking University, Beijing, China

Although serum amyloid A (SAA) is an excellent marker for coronary artery disease, its direct effect on atherogenesis *in vivo* is obscure. In this study we investigated the direct effect of SAA on promoting the formation of atherosclerosis in apolipoprotein E–deficient ($ApoE^{-/-}$) mice. Murine SAA lentivirus was constructed and injected into $ApoE^{-/-}$ mice intravenously. Then, experimental mice were fed a chow diet (5% fat and no added cholesterol) for 14 wks. The aortic atherosclerotic lesion area was larger with than without SAA treatment. With increased SAA levels, the plasma levels of interleukin-6 and tumor necrosis factor-α were significantly increased. Macrophage infiltration in atherosclerotic regions was enhanced with SAA treatment. A migration assay revealed prominent dose-dependent chemotaxis of SAA to macrophages. Furthermore, the expression of monocyte chemotactic protein-1 and vascular cell adhesion molecule-1 (VCAM-1) was upregulated significantly with SAA treatment. SAA-induced VCAM-1 production was detected in human aortic endothelial cells *in vitro*. Thus, an increase in plasma SAA directly accelerates the progression of atherosclerosis in $ApoE^{-/-}$ mice. SAA is not only a risk marker for atherosclerosis but also an active participant in atherogenesis.

Online address: http://www.molmed.org
doi: 10.2119/molmed.2011.00186

INTRODUCTION

Atherosclerosis is an important underlying pathologic condition of cardiovascular disease (CVD), the leading cause of morbidity and mortality worldwide (1). Because atherosclerosis is primarily a chronic inflammatory disease, clinical markers for inflammation are a useful indicator for identifying individuals at high risk of CVD. One marker is serum amyloid A (SAA), an acute-phase protein that is an excellent marker of inflammation and positively and significantly associated with prevalent CVD (2–4). However, whether an elevated plasma level of SAA is a consequence of inflammation or has a direct effect on atherogenesis is unknown.

SAA is one of the major acute-phase proteins in vertebrates (5). It is produced principally by the liver in response to acute inflammatory stimuli and its plasma concentration can increase by up to 100- to 1000-fold over the basal level (6). SAA exists both in an acute-phase form (A-SAA) and a constitutive form (C-SAA). The A-SAA form has major isoforms, SAA1 and SAA2, with primary structures that are 93% identical (98 of 104 amino acids). SAA1 predominates in plasma, where it functions as a major isotype (7,8). Accumulating evidence supports the involvement of SAA in atherogenesis. For example, when subcutaneously injected into mice, SAA may enhance the migration and adhesion of monocytes and polymorphonuclear leukocytes at the injection site (9), and SAA is deposited in murine atherosclerosis through all stages of lesion development (10). SAA increases the binding affinity of high-density lipoprotein (HDL) for macrophages and endothelial cells (11) and promotes cellular HDL cholesterol (HDL-C) metabolism through its effects on HDL-C ester uptake by scavenger receptor B-I (12). Murine SAA adenovirus injection resulted in decreased reverse cholesterol transport from macrophages to feces *in vivo* (13). Moreover, increased SAA levels mediated by a high-fat diet and cholesterol were found to be associated with increased atherosclerosis in mice (14), which provides a link between diet and inflammation. Recent studies have demonstrated that SAA can stimulate proteoglycan synthesis and induce endothelial dysfunction, which suggests a crucial role of SAA in atherosclerosis development (15,16).

**ZD and TW contributed equally to this paper.*

Address correspondence and reprint requests to *Fengshuang An or Cheng Zhang, Shandong University Qilu Hospital, Jinan, No. 107, Wen Hua Xi Road, Jinan, Shandong, 250012, P.R. China. Phone: +86531-82169257; Fax: +86531-86169356; E-mails: anfengshuang@hotmail.com, zhangcheng.1981@hotmail.com.*

Submitted May 24, 2011; Accepted for publication September 20, 2011; Epub (www.molmed.org) ahead of print September 21, 2011.

A series of *in vitro* experiments showed that SAA could modulate the activity and expression of multiple factors implicated in atherogenesis. For example, in vascular endothelial cells and monocytes, SAA greatly induced secretion of cytokines such as interleukin (IL)-1β, IL-6, IL-8, IL-10, tumor necrosis factor-α (TNF-α), and macrophage inflammatory protein 1α (17–19). SAA may also upregulate monocyte chemotactic protein-1 (MCP-1) in both human peripheral blood monocytes and umbilical vein endothelial cells (20,21). In addition, the role of SAA in rheumatoid arthritis, an inflammatory disease, has been explored (22).

Despite the numerous reported proatherogenic properties of SAA, we lack direct proof that SAA is an active participant in the atherosclerosis process *in vivo*. To investigate whether SAA is purely a risk marker for atherosclerosis or is also an active risk factor *in vivo*, we examined the effect of high-level expression of SAA on atherosclerosis development by using apolipoprotein E-deficient ($ApoE^{-/-}$) mice transfected with lentivirus to induce SAA overexpression. Findings from this study were consistent with a direct causal role of SAA in atherogenesis.

MATERIALS AND METHODS

Chemicals and Reagents

Because SAA1 is a major isotype of acute-phase protein SAA and may determine total SAA values (7), the lentiviral vector containing the coding sequence of the SAA1 gene was sourced commercially (Invitrogen, Shanghai, China). Recombinant human SAA protein (a consensus molecule of the SAA1 and SAA2, endotoxin level less than 0.1 ng/μg) was from Peprotec (Rocky Hill, NJ, USA). Goat anti–mouse antibody for SAA1 was from R&D Systems (Minneapolis, MN, USA). Rat anti–mouse monoclonal antibody for macrophages and rabbit anti–mouse polyclonal antibody for MCP-1 were from Abcam (Cambridge, MA, USA). Goat anti–mouse and human antibody for vascular cell adhesion molecule-1 (VCAM-1) was from Santa Cruz Biotechnology (Santa Cruz, CA, USA). We used a mouse SAA enzyme-linked immunosorbent assay (ELISA) kit from Invitrogen (Carlsbad, CA, USA). Mouse IL-6 and TNF-α ELISA kits were from eBioscience (San Diego, CA, USA).

Murine Studies

Male $ApoE^{-/-}$ mice (n = 120) were obtained from Peking University (Beijing, China). Mice were maintained under conditions of standard lighting (12:12-h light-dark cycle), temperature (20°C–22°C) and humidity (50%–60%) with food and water freely available. In total, 30 mice were fed a high-fat diet (16% fat and 0.25% cholesterol) for 12 wks, then another 90 animals were fed a chow diet (5% fat and no added cholesterol) for 14 wks for a subsequent study. The animal experimental protocol complied with the animal management rules of the Chinese Ministry of Health (document no. 55, 2001) and was approved by the Animal Care and Use Committee, Shandong University.

We randomly divided both diet groups of mice into three subgroups each. At age 8 wks, unanesthetized mice were injected intravenously with lentivirus-expressing mouse SAA1 (lenti-SAA group, high-fat diet group, n = 10; chow diet group, n = 30) at a total lentivector dose of 1×10^7 TU/mouse, a null lentivirus (lenti-null group, high-fat diet group, n = 10; chow diet group, n = 30) or saline (saline control group, high-fat diet group, n = 10; chow diet group, n = 30).

Collection of Blood Samples and Biological Measurements

At 14 wks after lentivirus injection, mice were anesthetized with pentobarbital injected intraperitoneally, and blood samples were taken by retro-orbital bleeding. Serum was separated by centrifugation at 4°C, and serum levels of SAA, IL-6 and TNF-α were detected by ELISA within 30 min. The levels of total cholesterol (TC), triglycerides (TG), HDL-C and low-density lipoprotein-cholesterol (LDL-C) were measured by use of an automatic biochemistry analyzer (Hitachi, Tokyo, Japan).

Tissue Harvesting and Quantification of Atherosclerosis

Mice were anesthetized by intraperitoneal pentobarbital injection, then perfused through the left ventricle with phosphate-buffered saline (PBS) under physiological pressure; the heart and aorta were removed and perfusion-fixed with 4% paraformaldehyde for histological and morphological staining or with PBS for real-time polymerase chain reaction (PCR) and Western blot analysis. Because the aortic arch region of $ApoE^{-/-}$ mice is the main part of the aorta that exhibits atherosclerotic lesion formation, atherosclerosis was evaluated by analysis of serial sections of the aortic sinus and by en face analysis of the aorta (23). Briefly, hearts were fixed in 4% paraformaldehyde overnight and then embedded in optimal cutting temperature compound. At least 50 serial cryosections 6-μm thick were cut, beginning at the junction of the left ventricle and the aorta. Sections were stained with hematoxylin and eosin (H&E). The lipid core was identified by Oil-Red-O staining. For en face analysis, the aorta was stripped of adventitia and dissected longitudinally from the iliac arteries to the aortic root, then branching vessels were removed. The paraformaldehyde-fixed aorta was pinned flat on a black surface, and the atherosclerotic lesion area was readily visualized with Oil-Red-O staining. Average lesion area was quantified by use of ImagePro-Plus software (Media Cybernetics).

Immunohistochemical Analysis

Immunohistochemical analysis involved the use of primary antibodies for macrophages (diluted 1:200) and MCP-1 (diluted 1:100). Briefly, cryosections were rehydrated in PBS (pH 7.4) and blocked with 3% H_2O_2 and 5% bovine serum albumin (BSA) for 20 min at room temperature. Tissue sections were incubated with primary antibodies overnight at 4°C and appropriate biotinylated secondary antibodies for 1 h at 37°C. Afterward, a

Table 1. Primer sequences for real-time PCR.

Species and symbol	Forward primer	Reverse primer
Murine		
MCP-1	TTAAAAACCTGGATCGGAACCAA	GCATTAGCTTCAGATTTACGGGT
VCAM-1	AGTTGGGGATTCGGTTGTTCT	CCCCTCATTCCTTACCACCC
β-Actin	AGTGTGACGTTGACATCCGTA	GCCAGAGCAGTAATCTCCTTCT
TBP	CCTTGTACCCTTCACCAATGAC	ACAGCCAAGATTCACGGTAGA
GAPDH	AGGTCGGTGTGAACGGATTTG	GGGGTCGTTGATGGCAACA
Human		
VCAM-1	GCTGCTCAGATTGGAGACTCA	CGCTCAGAGGGCTGTCTATC
β-Actin	CATGTACGTTGCTATCCAGGC	CTCCTTAATGTCACGCACGAT
TBP	AGTTCTGGGATTGTACCGCAG	GCACGAAGTGCAATGGTCT
GAPDH	AAGGTGAAGGTCGGAGTCAAC	GGGGTCATTGATGGCAACAATA

3,3′-diaminobenzidine staining kit (ZSGB-Bio, Beijing, China) was used to visualize the primary antibody, then sections were rinsed in water and counterstained with hematoxylin to detect cell nuclei. Data were analyzed by use of ImagePro-Plus software.

Immunofluorescence

Cryosections were blocked with 5% BSA for 20 min at room temperature. Then, sections were incubated with primary antibodies against SAA1 (diluted 1:200), macrophages (diluted 1:200) and VCAM-1 (diluted 1:100) overnight at 4°C and then for 1 h at 37°C with an appropriate secondary antibody. DyLight 549–conjugated donkey anti–goat IgG (Jackson ImmunoResearch, West Grove, PA, USA), Cy2-conjugated donkey anti–goat IgG (Jackson ImmunoResearch) and FITC-conjugated goat anti–rat IgG (Santa Cruz Biotechnology) were used as secondary antibodies. A drop of prolong gold antifade reagent with DAPI (Invitrogen) was used to seal coverslips. Images were acquired by laser scanning confocal microscopy (LSM710, Carl Zeiss, Germany). Data were analyzed by use of ImagePro-Plus software.

Cell Culture and Western Blot Analysis

Human aortic endothelial cells (HAECs) were obtained from American Type Culture Collection (Manassas, VA, USA) and cultured in endothelial culture medium (ScienCell, San Diego, CA, USA) supplemented with 5% fetal bovine serum (FBS). Cells between passages three and five were used. HAECs were stimulated with 20 μg/mL recombinant human SAA protein for various times, then proteins were extracted and separated on 10% sodium dodecyl sulfate–polyacrylamide gel, and blotted onto a polyvinylidene difluoride membranes (Pierce, Rockford, IL, USA), which were incubated with 5% nonfat dry milk in TBS-T [20 mmol/L Tris-HCl (pH 8.0), 8 g/L NaCl, and 0.1% Tween 20] at room temperature for 2 h, then with goat anti–human antibody for VCAM-1 at 4°C overnight and washed with TBS-T. Antigen-antibody complexes were visualized after incubation with horseradish peroxidase–conjugated rabbit anti–goat IgG antibody (1:10000) with use of the SuperSignal West Pico enhanced chemiluminescence kit (Pierce). Immunoreactive bands were quantified by use of the densitometer analysis system Flurochem 9900-50 (α Innotech, Santa Clara, CA, USA). The expression level of the sample was indicated as a ratio of sample to β-actin.

Quantitative Real-Time PCR

Total RNA was extracted from frozen aortic specimens or HAECs by use of Trizol (Invitrogen) according to the manufacturer's instructions. The concentration of total RNA was quantified by spectrophotometry and reverse transcribed with use of the M-MLV (Moloney murine leukemia virus) Reverse Transcriptase System (Fermentas, Shenzhen, China) and oligo (dT). Total cDNA was amplified by use of Light-Cycler-FastStart DNA Master SYBR Green I (TaKaRa Biotechnology, Dalian, China). It was very important to select the appropriate reference genes in the real-time PCR. Thus, a reference gene group including *β-actin*, *TATA box binding protein* (*TBP*) and *GAPDH* was chosen for both *in vivo* and *in vitro* studies according to the relevant references (18,21,24–27). In addition, the geometric mean of the expression of the reference genes was used to confirm the robustness of experimental data (28). Real-time PCR was carried out by using the primers listed in Table 1. The specificity of products generated for each set of primers was examined with the use of a melting curve and gel electrophoresis. The relative expression levels of each target gene were normalized to the mRNA of the internal standard genes.

Migration Assay

The migration assay involved use of a modified Boyden chamber containing polycarbonate inserts with 8-μm pores (BD Biosciences, Oxford, UK). To detect murine macrophage chemotaxis to SAA, the murine SAA1 lentivirus was transfected into HEK 293 cells (ATCC). Cells were cultured in Dulbecco´s modified Eagle's medium (DMEM) (Invitrogen) supplemented with 10% FBS for 72 h, then cell-free supernatants that contained a large amount of murine SAA1 protein were collected and diluted for different times with DMEM to form a concentration gradient (1:5, 1:10, 1:50). To assess macrophage migration, 1×10^5 RAW264.7 murine macrophages (ATCC) were loaded in the upper chamber, and the lower chamber contained different concentrations of murine SAA1 protein diluted with DMEM. After incubation for 8 h at 37°C in a 5% CO_2 incubator, nonmigrating cells were removed from the upper surface by gentle scrubbing. Migrated cells attached to the lower membrane were fixed with 1% glutaraldehyde and stained with 0.1% crystal violet. To assess the mean number of migrating cells, cells were counted in five random fields.

Statistical Analysis

SPSS for Windows v16.0 (SPSS Inc, Chicago, IL, USA) was used for statistical

Table 2. Characteristics of mice fed a chow diet with and without lenti-SAA.[a]

Chow diet	Saline control (n = 30)	Lenti-null (n = 30)	Lenti-SAA (n = 30)
Body weight, g	28.2 ± 1.2	28.1 ± 1.4	27.9 ± 0.9
TG, mmol/L	0.5 ± 0.1	0.5 ± 0.1	0.4 ± 0.1
TC, mmol/L	15.2 ± 2.4	14.9 ± 2.1	15.7 ± 2.3
HDL-C, mmol/L	1.5 ± 0.3	1.7 ± 0.3	1.6 ± 0.3
LDL-C, mmol/L	6.2 ± 1.3	6.7 ± 1.4	6.4 ± 1.6
SAA, μg/mL	8.3 ± 2.4	8.5 ± 2.8	35.5 ± 9.6[b]
IL-6, pg/mL	135.8 ± 15.7	132.4 ± 21.5	360.1 ± 134.6[b]
TNF-α, pg/mL	11.2 ± 3.6	11.1 ± 3.0	43.4 ± 15.8[b]

[a]Data are mean ± SD.
[b]$P < 0.01$ compared with lenti-null group.

analysis. Results were expressed as mean ± SD. The normal distribution of our data was checked by use of the SPSS program. Data were assessed by one-way ANOVA or Student *t* test between two groups. $P < 0.05$ was considered statistically significant.

RESULTS

Body Weight and Measurement of Plasma Variables

ApoE$^{-/-}$ mice fed a chow diet did not differ in body weight, activity, behavior, or lipid levels by treatment (Table 2). Therefore, we excluded the influence of lipid levels on atherosclerosis in this study. The plasma levels of SAA were higher for the lenti-SAA group than the lenti-null and saline control groups, so the SAA1 lentivirus was efficiently transfected *in vivo* (Table 2). The lenti-null and saline control groups did not differ in plasma levels of IL-6 or TNF-α, so the injection of the lentivirus vector was safe and did not induce inflammatory responses. Most importantly, with elevated SAA levels, the plasma levels of IL-6 and TNF-α were significantly higher in the lenti-SAA than the lenti-null group, which agreed with previous *in vitro* studies (18,19).

Increased Plasma SAA Level Directly Promotes Atherosclerotic Lesions with the Chow Diet

Atherosclerotic lesion involvement in ApoE$^{-/-}$ mice was confined mainly to the aortic arch region throughout the entire experiment. With a high-fat diet, the lenti-SAA and lenti-null groups did not differ in plaque formation (Figure 1), but with a chow diet, all lenti-SAA mice showed plaque formation in the aortic arch (Figure 2), with no plaque found in 7 of 30 mice in the lenti-null group, and only mild lesions found in the other 23 mice (76.67%). By using en face analysis of the aorta, we calculated total atherosclerotic lesion area as an indicator to evaluate the level of atherogenesis (Figure 2A). Lesion area was significantly larger for the lenti-SAA than the lenti-null group (7.74% ± 2.35% versus 1.69% ± 1.35%, $P < 0.01$; Figure 2B). The atherogenesis level at the aortic sinus was evaluated by Oil-Red-O and H&E staining according to the ratio of total atherosclerotic lesion area to aortic lumen area (Figure 2C). The mean lesion sizes at the aortic sinus were greater for the lenti-SAA than the lenti-null group (18.14 ± 4.17 versus 6.06 ± 4.23, $P < 0.05$; Figure 2D). Thus, we used chow-fed mice for subsequent experiment.

Increase in Plasma SAA Level is Associated with Macrophage Accumulation in Atherosclerotic Regions

Immunohistochemical analysis showed a greater increase in the accumulation of macrophages for the lenti-SAA than the lenti-null group (Figure 3A). Because SAA is a classic chemoattractant to peripheral blood leukocytes, we ob-

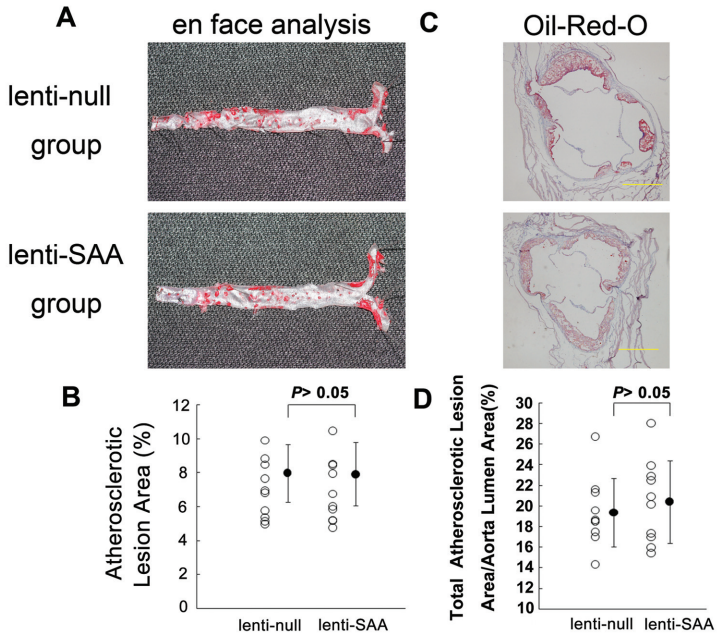

Figure 1. Quantification of atherosclerosis in mice fed a high-fat diet. (A) En face analysis of aortas. Atherosclerotic lesions were identified by Oil-Red-O staining. (B) Total atherosclerotic lesion area indicating level of atherogenesis. (C) Oil-Red-O staining of aortic sinus cryosections (bar = 500 μm). (D) Ratio of total atherosclerotic lesion area to aorta lumen area indicating mean size of atherosclerotic plaque. Data are mean ± SD. *$P > 0.05$ compared with lenti-null group (n = 10 for both groups).

served the colocalization of SAA with macrophages in lesions on aortic cryosections. The distribution of macrophages was consistent with SAA protein localization (Figure 3B). To confirm the association of SAA protein and macrophage distribution *in vitro*, we performed a migration assay and found prominent dose-dependent SAA chemotaxis to macrophages (Figure 3C).

SAA Induces MCP-1 Secretion in Atherosclerotic Plaque

Because MCP-1 is a key molecule regulating chemotactic migration of macrophages, we observed the expression of MCP- *in vivo* by use of immunohistochemical analysis. MCP-1 secretion was increased with an elevated level of plasma SAA (Figures 4A, B), which was confirmed by real-time PCR (Figure 4C).

SAA Upregulates VCAM-1 Production in Atherosclerotic Lesions and In Vitro

Immunofluorescence analysis revealed upregulated VCAM-1 expression *in vivo* in the lenti-SAA group compared with the lenti-null group (Figures 5A, B). VCAM-1 mRNA expression results agreed with protein-level results (Figure 5C). To further demonstrate the role of SAA on VCAM-1 expression *in vitro*, Western blot analysis of VCAM-1 expression in HAECs stimulated with recombinant human SAA (20 μg/mL) for various times showed time-dependent induction of VCAM-1 production (Figure 5D). Real-time PCR of the mRNA expression confirmed these results, which suggested that SAA-induced VCAM-1 synthesis requires transcriptional activation (Figure 5E). In addition, VCAM-1 expression was dose-dependently induced in HAECs treated with different concentrations of SAA (Figure 5F).

DISCUSSION

We report a novel direct effect of SAA in atherogenesis in mice, in that an increased plasma level of SAA can accelerate the progression of atherogenesis. Macrophages were accumulated in atherosclerotic regions of lenti-

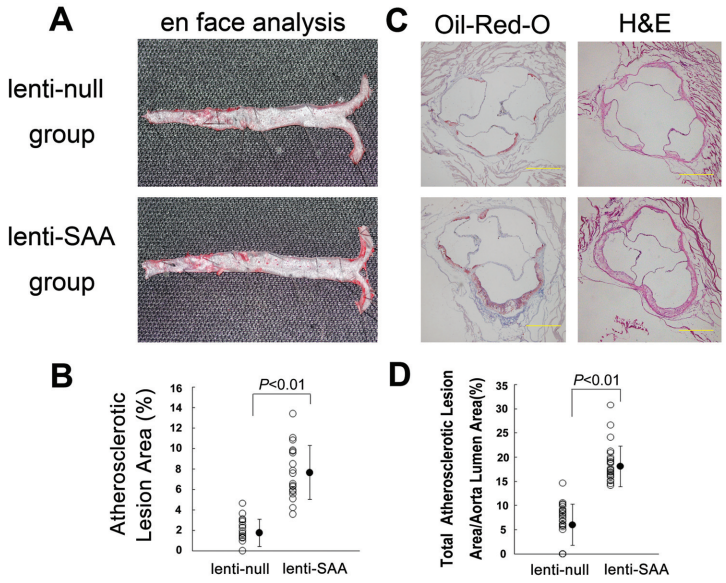

Figure 2. Quantification of atherosclerosis in mice fed a chow diet. (A) En face analysis of aortas. Atherosclerotic lesions were identified by Oil-Red-O staining. (B) Total atherosclerotic lesion area indicating level of atherogenesis (n = 18 for both groups). (C) H&E and Oil-Red-O staining of aortic sinus cryosections (bar = 500 μm). (D) The ratio of total atherosclerotic lesion area to aorta lumen area indicating mean size of atherosclerotic plaque. Data are mean ± SD. *$P < 0.01$ compared with the lenti-null group (n = 25 for both groups).

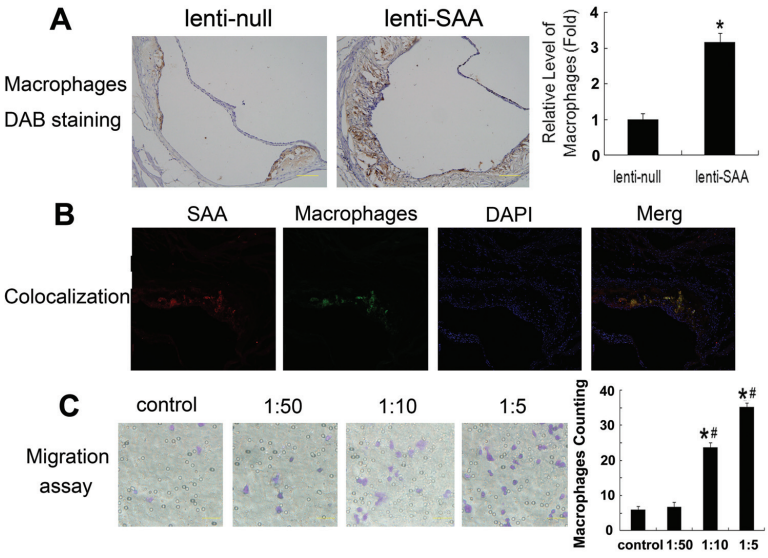

Figure 3. Elevated plasma SAA level induces the accumulation of macrophages in atherosclerotic regions of chow-fed mice. (A) Representative images by immunohistochemistry staining for macrophages (brown) (bar = 100 μm). *$P < 0.01$ compared with the lenti-null group (n = 10 for both groups). (B) The colocalization of SAA (red) with macrophages (green) by immunofluorescence analysis (Magnification 100×). (C) Migration assay of chemotaxis of SAA to macrophages by dilution dose of SAA with DMEM. Data are mean ± SD from 5 separate fields in each sample from 3 independent experiments (bar = 50 μm). *$P < 0.05$ versus control group and $^{\#}P < 0.05$ versus 1:50 group.

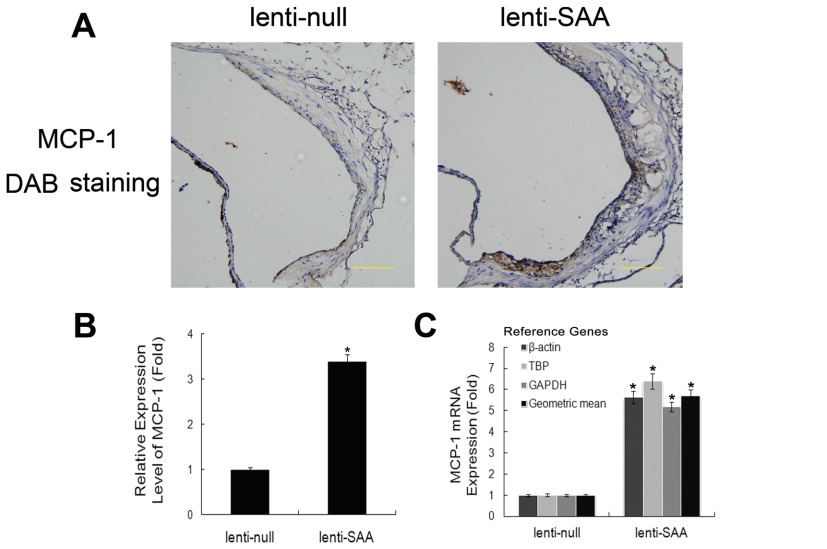

Figure 4. SAA upregulates MCP-1 secretion in atherosclerotic plaque of chow-fed mice. (A, B) Immunohistochemistry staining and quantification of MCP-1 (brown, bar = 100 μm; n = 10 for both groups). (C) Real-time PCR analysis of mRNA expression of MCP-1. Relative expression was normalized to that of reference genes *β-actin*, *TBP* and *GAPDH*. Geometric mean of reference gene expressions was used to confirm the robustness of experimental data. Data are mean ± SD. **P* < 0.01 compared with the lenti-null group (n = 12 for both groups).

SAA–treated mice. In addition, MCP-1 expression in aortas was upregulated with the increased plasma level of SAA. These data *in vivo* agree with previous results *in vitro* (20,21). SAA induced VCAM-1 expression in HAECs, thus increasing the formation of atherosclerotic plaque by enhancing the binding of leukocytes to HAECs in lesion regions. Plasma levels of IL-6 and TNF-α were significantly increased with elevated levels of plasma SAA *in vivo*. All of these results demonstrate a key role of SAA as a direct participant in the process of inflammation and leukocyte recruitment, adhesion and migration, which ultimately accelerate the formation of atherosclerosis. SAA is not merely a locally expressed acute-phase or bystander protein but also a key regulator in the pathology of atherosclerosis.

Under normal conditions the production of SAA in the acute-phase response is accompanied by a marked increase in SAA, which is then catabolized by the liver, leading to lower levels. However, in chronic diseases SAA levels can be persistently elevated. Therefore, in chronic inflammatory diseases SAA may be derived from some other tissues such as adipose tissue. Thus, we constructed a lentiviral vector containing the coding sequence of the *SAA1* gene to imitate persistent overexpression of SAA1. Increased SAA expression in subcutaneous white adipose tissue can result in increased circulatory levels of SAA (29). The epidemic of obesity is accompanied by an increase in atherosclerotic diseases and may have a close association with SAA levels (30). The increase in adipose-derived SAA in obesity may be a mechanistic link between obesity and accelerated atherosclerosis.

In the present study, the proinflammatory effects of SAA on increasing the plasma levels of IL-6 and TNF-α *in vivo* were consistent with those of previous studies *in vitro* (18). Because the plasma levels of IL-6 and TNF-α are predominant indicators of inflammation and both are activists in the inflammatory response (31,32), SAA is strongly implicated as a powerful and rapid inducer of proinflammatory cytokines, thus contributing to the progression of atherosclerosis. In addition, a comparison of plasma levels of IL-6 and TNF-α in lenti-null and saline control groups revealed the safety of lentivirus vector injection. Therefore, we could focus on the difference between the lenti-SAA group and lenti-null group.

Atherosclerosis is an inflammatory disease characterized by dynamic interactions between cells in the arterial wall, including endothelial cells and macrophages (33). During the pathogenesis of atherogenesis, persistent macrophage infiltration is crucial as a response to invasion of pathogenic lipoproteins in arterial walls (34). Thus, the deposition of macrophages in atherosclerotic plaque should be detected. Our findings both *in vivo* and *in vitro* support those of previous studies demonstrating that SAA is a bioactive chemotaxin for monocytes/macrophages (35,36) and can upregulate chemotactic cytokines including MCP-1 and TNF-α (37). In addition, SAA is an apolipoprotein that can bind to HDL and LDL (11,38), which, along with the accumulation of SAA protein, attracts phagocytes to lesion regions so that SAA/HDL or SAA/LDL are phagocytized rapidly by macrophages. However, with this process, the number of foam cells will increase and promote the formation of atherosclerotic plaque. We showed increased accumulation of macrophages in the lenti-SAA group, and colocalization of SAA with macrophages was confirmed in lesions on aortic cryosections. Furthermore, migration of inflammatory cells is a key step in the early event of atherogenesis and is mediated by the presence of cell adhesion molecules, including VCAM-1, on the vascular endothelium (39). We demonstrated that SAA-induced VCAM-1 expression promoted adherence of leukocytes to HAECs in atherosclerotic lesions. In combination with its chemotactic ability, SAA indeed exerts a direct role in atherogenesis.

Although the influence of plasma lipids on atherogenesis was ruled out to

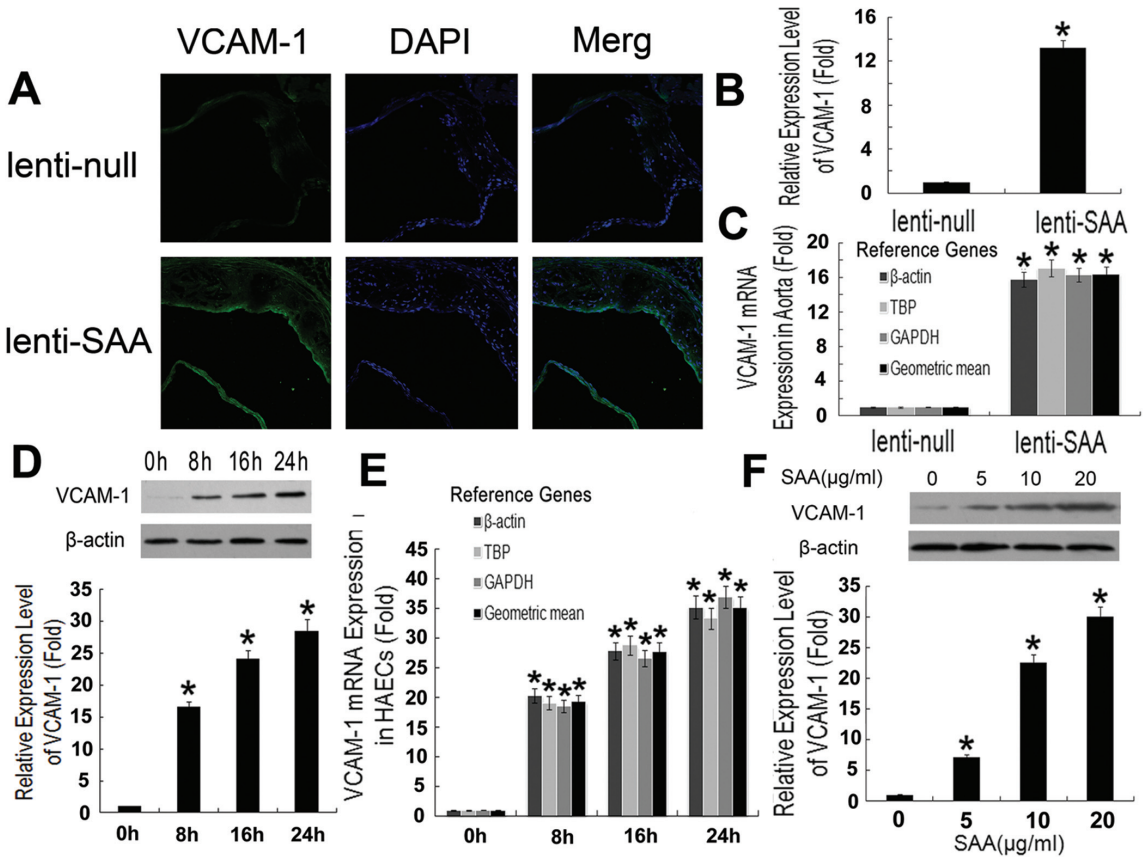

Figure 5. SAA induces VCAM-1 production in atherosclerotic lesions of chow-fed mice and *in vitro*. (A, B) Expression of VCAM-1 (green) by immunofluorescence analysis and quantification (magnification 200×; n = 10 for both groups). (C) Real-time PCR analysis of VCAM-1 mRNA expression in aortas (n = 12 for both groups). Relative expression was normalized to that of a reference gene group including *β-actin*, *TBP* and *GAPDH*. Geometric mean of reference gene expressions was used to confirm the robustness of experimental data. Data are mean ± SD. **P* < 0.01 compared with lenti-null group. (D) and (E) HAECs were stimulated with recombinant human SAA (20 μg/mL) for various times. Western blot and real-time PCR analysis of VCAM-1 protein and mRNA expression. (F) Human aortic endothelial cells were treated with different concentrations of SAA for 24 h. Protein expression of VCAM-1 was investigated with Western blot analysis. Data are mean ± SD from 3 independent experiments performed in duplicate. **P* < 0.05 compared with control.

emphasize the direct independent effects of SAA in this study, obesity and hyperlipidemia are the major reasons for an elevation in plasma SAA concentration in the chronic physiological condition, with SAA considered an important adipokine (19). For our group of mice fed a high-fat diet for 12 wks, we found no difference in lesion area between the lenti-null and lenti-SAA groups (see Figure 1), despite a higher plasma SAA level for the lenti-SAA group (71.6 ± 12.7 versus 86.5 ± 13.2 μg/mL). The proatherogenic role of SAA lentivirus may have been masked by hyperlipidemia. Therefore, to highlight the independent effects of SAA on atherogenesis, we investigated mice given a chow diet and found a significant difference in lesion area between the two groups.

In conclusion, we provided the first *in vivo* evidence that an elevated plasma level of SAA can accelerate the progression of atherosclerosis directly and independently. SAA is an active participant in the process of atherogenesis by inducing expression of inflammatory cytokines and promoting the recruitment, adhesion and migration of leukocytes, thus contributing to the link between obesity and atherosclerosis. These findings may be helpful in designing novel therapeutic strategies against obesity-associated atherosclerosis.

ACKNOWLEDGMENTS

This study was supported by the National 973 Basic Research program (2009CB521904), the grant of Natural Science Foundation of Shandong Province (Y2007C074) and Independent Innovation Foundation of Shandong University (2009DX004).

DISCLOSURE

The authors declare that they have no competing interests as defined by *Molecular Medicine*, or other interests that

might be perceived to influence the results and discussion reported in this paper.

REFERENCES

1. Libby P. (2002) Inflammation in atherosclerosis. *Nature.* 420:868–74.
2. Jousilahti P, Salomaa V, Rasi V, Vahtera E, Palosuo T. (2001) The association of c-reactive protein, serum amyloid a and fibrinogen with prevalent coronary heart disease—baseline findings of the PAIS project. *Atherosclerosis.* 156:451–6.
3. Johnson BD, *et al.* (2004) Serum amyloid A as a predictor of coronary artery disease and cardiovascular outcome in women: the National Heart, Lung, and Blood Institute-Sponsored Women's Ischemia Syndrome Evaluation (WISE). *Circulation.* 109:726–32.
4. Schillinger M, *et al.* (2005) Inflammation and Carotid Artery—Risk for wAtherosclerosis Study (ICARAS). *Circulation.* 111:2203–9.
5. Uhlar CM, Whitehead AS. (1999) Serum amyloid A, the major vertebrate acute-phase reactant. *Eur. J. Biochem.* 265:501–23.
6. Urieli-Shoval S, Linke RP, Matzner Y. (2000) Expression and function of serum amyloid A, a major acute-phase protein, in normal and disease states. *Curr. Opin. Hematol.* 7:64–9.
7. Xu Y, Yamada T, Satoh T, Okuda Y. (2006) Measurement of serum amyloid A1 (SAA1), a major isotype of acute phase SAA. *Clin. Chem. Lab. Med.* 44:59–63.
8. Yamada T, Wada A, Itoh Y, Itoh K. (1999) Serum amyloid A1 alleles and plasma concentrations of serum amyloid A. *Amyloid.* 6:199–204.
9. Badolato R, *et al.* (1994) Serum amyloid A is a chemoattractant: induction of migration, adhesion, and tissue infiltration of monocytes and polymorphonuclear leukocytes. *J. Exp. Med.* 180:203–9.
10. O'Brien KD, *et al.* (2005) Serum amyloid A and lipoprotein retention in murine models of atherosclerosis. *Arterioscler. Thromb. Vasc. Biol.* 25:785–90.
11. Hayat S, Raynes JG. (2000) Acute phase serum amyloid A protein increases high density lipoprotein binding to human peripheral blood mononuclear cells and an endothelial cell line. *Scand. J. Immunol.* 51:141–6.
12. van der Westhuyzen DR, Cai L, de Beer MC, de Beer FC. (2005) Serum amyloid A promotes cholesterol efflux mediated by scavenger receptor B-I. *J. Biol. Chem.* 280:35890–5.
13. Annema W, *et al.* (2010) Myeloperoxidase and serum amyloid A contribute to impaired in vivo reverse cholesterol transport during the acute phase response but not group IIA secretory phospholipase A(2). *J. Lipid. Res.* 51:743–54.
14. Lewis KE, *et al.* (2004) Increase in serum amyloid a evoked by dietary cholesterol is associated with increased atherosclerosis in mice. *Circulation.* 110: 540–5.
15. Wilson PG, Thompson JC, Webb NR, de Beer FC, King VL, Tannock LR. (2008) Serum amyloid A, but not C-reactive protein, stimulates vascular proteoglycan synthesis in a pro-atherogenic manner. *Am. J. Pathol.* 173:1902–10.
16. Wang X, Chai H, Wang Z, Lin PH, Yao Q, Chen C. (2008) Serum amyloid A induces endothelial dysfunction in porcine coronary arteries and human coronary artery endothelial cells. *Am. J. Physiol. Heart. Circ. Physiol.* 295:H2399–408.
17. Furlaneto CJ, Campa A. (2000) A novel function of serum amyloid A: a potent stimulus for the release of tumor necrosis factor-alpha, interleukin-1beta, and interleukin-8 by human blood neutrophil. *Biochem. Biophys. Res. Commun.* 268:405–8.
18. Song C, *et al.* (2009) Serum amyloid A induction of cytokines in monocytes/macrophages and lymphocytes. *Atherosclerosis.* 207:374–83.
19. Yang RZ, *et al.* (2006) Acute-phase serum amyloid A: an inflammatory adipokine and potential link between obesity and its metabolic complications. *P.L.o.S. Med.* 3:e287.
20. Lee HY, *et al.* (2008) Serum amyloid A induces CCL2 production via formyl peptide receptor-like 1-mediated signaling in human monocytes. *J. Immunol.* 181:4332–9.
21. Lee HY, Kim SD, Shim JW, Yun J, Kim K, Bae YS. (2009) Activation of formyl peptide receptor like-1 by serum amyloid A induces CCL2 production in human umbilical vein endothelial cells. *Biochem. Biophys. Res. Commun.* 380:313–7.
22. Mullan RH, *et al.* (2006) Acute-phase serum amyloid A stimulation of angiogenesis, leukocyte recruitment, and matrix degradation in rheumatoid arthritis through an NF-kappaB-dependent signal transduction pathway. *Arthritis Rheum.* 54:105–14.
23. Baglione J, Smith JD. (2006) Quantitative assay for mouse atherosclerosis in the aortic root. *Methods Mol. Med.* 129:83–95.
24. Martino A, *et al.* (2011) Selection of reference genes for normalization of real-time PCR data in minipig heart failure model and evaluation of TNF-alpha mRNA expression. *J. Biotechnol.* 153:92–9.
25. Xu L, Ma X, Cui B, Li X, Ning G, Wang S. (2011) Selection of reference genes for qRT-PCR in high fat diet-induced hepatic steatosis mice model. *Mol. Biotechnol.* 48:255–62.
26. Witting PK, *et al.* (2011) The acute-phase protein serum amyloid A induces endothelial dysfunction that is inhibited by high-density lipoprotein. *Free Radic. Biol. Med.* 51:1390–8.
27. Gibson FC 3rd, *et al.* (2004) Innate immune recognition of invasive bacteria accelerates atherosclerosis in apolipoprotein E-deficient mice. *Circulation.* 109:2801–6.
28. Vandesompele J, *et al.* (2002) Accurate normalization of real-time quantitative RT-PCR data by geometric averaging of multiple internal control genes. *Genome. Biol.* 3:RESEARCH0034.
29. Poitou C, *et al.* (2005) Serum amyloid A: production by human white adipocyte and regulation by obesity and nutrition. *Diabetologia.* 48:519–528.
30. Zhao Y, *et al.* (2010) Association between serum amyloid A and obesity: a meta-analysis and systematic review. *Inflamm. Res.* 59:323–34.
31. Schuett H, Luchtefeld M, Grothusen C, Grote K, Schieffer B. (2009) How much is too much? Interleukin-6 and its signaling in atherosclerosis. *Thromb. Haemost.* 102:215–22.
32. Maksimowicz-McKinnon K, Bhatt DL, Calabrese LH. (2004) Recent advances in vascular inflammation: C-reactive protein and other inflammatory biomarkers. *Curr. Opin. Rheumatol.* 16:18–24.
33. Zouridakis E, Avanzas P, Arroyo-Espliguero R, Fredericks S, Kaski JC. (2004) Markers of inflammation and rapid coronary artery disease progression in patients with stable angina pectoris. *Circulation.* 110:1747–53.
34. Li AC, Glass CK. (2002) The macrophage foam cell as a target for therapeutic intervention. *Nat. Med.* 8:1235–42.
35. Su SB, *et al.* (1999) A seven-transmembrane, G protein-coupled receptor, FPRL1, mediates the chemotactic activity of serum amyloid A for human phagocytic cells. *J. Exp. Med.* 189:395–402.
36. Badolato R, *et al.* (1995) Serum amyloid A induces calcium mobilization and chemotaxis of human monocytes by activating a pertussis toxin-sensitive signaling pathway. *J. Immunol.* 155:4004–10.
37. Hatanaka E, Furlaneto CJ, Ribeiro FP, Souza GM, Campa A. (2004) Serum amyloid A-induced mRNA expression and release of tumor necrosis factor-alpha (TNF-alpha) in human neutrophils. *Immunol. Lett.* 91:33–7.
38. Ogasawara K, *et al.* (2004) A serum amyloid A and LDL complex as a new prognostic marker in stable coronary artery disease. *Atherosclerosis.* 174:349–56.
39. Preiss DJ, Sattar N. (2007) Vascular cell adhesion molecule-1: a viable therapeutic target for atherosclerosis? *Int. J. Clin. Pract.* 61:697–701.